

The correction of Inelastic Neutron Scattering data of organic samples using the Average Functional Group Approximation

Enrico Preziosi¹, Carla Andreani¹, Giovanni Romanelli^{1,*}, and Roberto Senesi¹

¹Physics Department and NAST Centre, Università degli Studi di Roma “Tor Vergata”, Via della Ricerca, Scientifica 1, 00133, Roma, Italy

Abstract. The use of the Average Functional Group Approximation for self-shielding corrections at inelastic neutron spectrometers is discussed. By taking triptindane as a case study, we use the above-mentioned approximation to simulate a synthetic dynamic structure factor as measured on an indirect-geometry spectrometer, as well as the related total scattering cross section as a function of incident neutron energy and sample temperature, and the transmission spectra depending on the sample thickness. These quantities, obtained in a consistent way from the Average Functional Group Approximation, are used to calculate the energy-dependent self-shielding correction affecting the sample under investigation. The impact on the intensities of low-energy vibrational modes is discussed, showing that at typical experimental conditions the sample-dependent attenuation factor is about 15% higher compared to the correction at higher energies.

1 Introduction

Inelastic Neutron Scattering (INS) and Quasi-Elastic Neutron Scattering (QENS) are well-established experimental techniques allowing to study the atomic-scale dynamics of condensed-matter systems [1–3]. The investigation of hydrogenous compounds through these techniques has found a naturally successful application, since hydrogen (¹H) has the largest bound scattering cross section (82.03 barn) among the elements of the periodic table [4].

Neutron data from hydrogen-containing organic systems collected in INS and, to a lesser extent, QENS experiments, can be subject to non-trivial and sample-dependent attenuation corrections related to the total scattering cross section at thermal neutron energy, also referred to as Thermal neutron Cross Section (TCS). These act as attenuation functions whose intensity can change up to a factor of 4 in the neutron energy range between units and hundreds of meV. As the TCS depends upon temperature as well as upon the structure and dynamics of the system – i.e., the ultimate objectives of the experiment itself – the correction of the experimental spectra becomes, in principle, a very challenging task. The significant change of the TCS affects the INS peak intensities in an energy-dependent way, therefore complicating the accurate comparison with state-of-the-art computer simulations as well as other experiments at different experimental conditions.

Knowing TCSs of the materials of interest is a challenging task, following the dependencies on the molecular structure, dynamics, and temperature. In addition, it is quite uncommon to have the possibility to obtain them from experimental measurements over a broad range of neutron energies, since specific instrumentation (e.g. the

VESUVIO beamline at ISIS Neutron and Muon Source, UK [5]) is required. For this reason, experimentally obtained and tabulated TCS are available for just few systems. In order to overcome the impossibility of direct measurements, it is possible to retrieve TCS by calculations from simplified models [6, 7], from molecular dynamics [8], as well as from ab initio calculations [9–13].

In this context, a wide experimental campaign of measurements has been started at the VESUVIO spectrometer [14–16] to investigate TCS of alcohols [17], organic systems [18], water [18, 19] or neutron moderators [20–23]. In particular, in Ref.[24], a new approach for the modelling of TCSs was developed, referred to the Average Functional Group Approximation (AFGA), specifically designed for organic hydrogen-containing systems and based on the incoherent approximation. Within this model, the TCS of large macromolecules and polymers can be estimated, for which a rigorous phonon-based calculation would be prohibitive.

TCS information can be used to correct INS measurements, as presented in [25, 26], via a post-processing procedure referred to as InSCorNorm. This procedure, requiring the knowledge of the energy-dependent TCS of the sample under investigation, allows the correction of the measurements for the experimental conditions, so as to make easier the comparison of the INS experimental spectra with single-molecule or periodic DFT calculations. Moreover, the InSCorNorm algorithm allows to express the experimental INS data on an absolute intensity scale, removing any arbitrary procedure, once the value of the average kinetic energy is known.

Here, we show how the InSCorNorm algorithm in Ref. [25] can be easily adapted so as to take as an in-

*e-mail: giovanni.romanelli@uniroma2.it

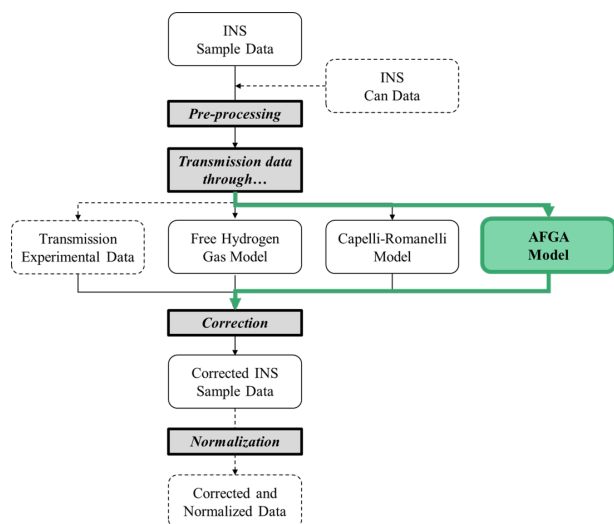


Figure 1. Workflow highlighting the addition of the AFGA method in the INSCorNorm algorithm. Adapted from [25].

put an AFGA-simulated TCS [24] when the direct measurement of the experimental one is not possible. In Figure 1 the workflow of the INSCorNorm algorithm is integrated with the AFGA method that allows to obtain TCSs of compounds when transmission measurements are not available. With respect to the other methods integrated in the standard INSCorNorm algorithm (namely, Free Hydrogen Gas Model and the model by Capelli and Romanelli [18], see Figure 1), the addition of AFGA Model provides a sample-specific TCS for organic and biological compounds. We take as an example of application triptindane, a molecule at the base of a series of compounds of interest for the industry of hydrogen storage and catalysis [27, 28].

2 Materials and Methods

The triptindane molecule ($C_{23}H_{18}$) was rationalised as composed of 3 CH_2 aliphatic groups and 12 aromatic CH groups. The average hydrogen-projected Vibrational Densities of States (VDoSs), g_H , of a given hydrogen atom in the molecule was calculated as

$$g_H = \frac{1}{18} (6 \cdot g_{CH_2} + 12 \cdot g_{CH,aro}) \quad (1)$$

where g_{CH_2} and $g_{CH,aro}$ correspond to the average hydrogen-projected VDoS of a single hydrogen atom in a CH_2 group or aromatic CH group, respectively. The VDoS of specific functional groups as calculated within the AFGA were taken from Ref.[24] (see Supplementary Information therein), and g_H was used to calculate the TCS of the molecule according to the AFGA model. Moreover, we pushed the model a step forward to calculate the double differential scattering cross section as follows. Using such VDoSs as an input and using the multi-phonon expansion (in particular Eqs. 3–7 in Ref.[24]), we calculated the synthetic dynamic scattering function $S(Q, \Delta E)$, as a function of the neutron momentum and energy transfers,

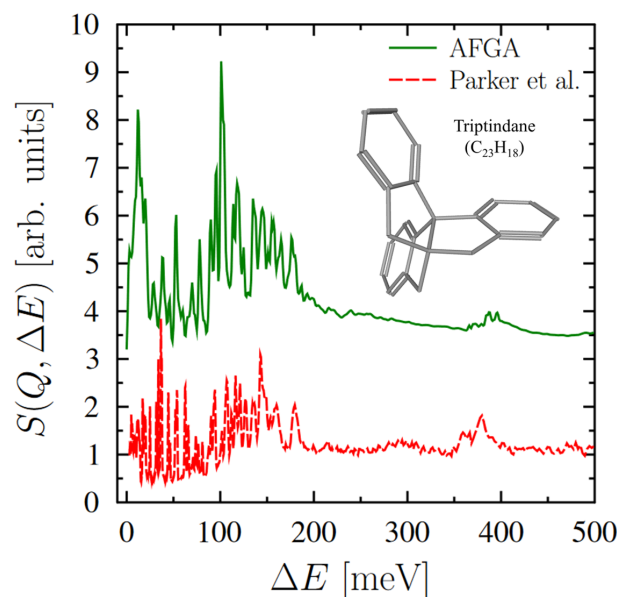


Figure 2. INS spectra of triptindane from Ref[30] (red dashed line) and synthetic spectrum obtained using the AFGA model (green solid line) as a function of the neutron energy transfer. The latter is vertically shifted for the sake of clarity. The figure also shows the structure of the molecule, from [33].

Q and ΔE , at a sample temperature of 20 K. We considered an indirect-geometry neutron spectrometer, as well as a scattering angle and final energy equal to those available for the forward-scattering detectors on the TOSCA spectrometer at ISIS [29]. The results, reported in Figure 2, is compared to the experimental data recently measured on TOSCA [30] obtained from the INS TOSCA database [31]. The comparison shows an overall qualitative agreement of the two spectra – a very good result from a model aimed at accurately reproducing total cross sections rather than double-differential ones. However, an interesting feature of the synthetic spectrum is that the low-energy modes seem to be clearly more intense compared to the experimental ones. At the end of our discussion we will relate such difference, at least partially, to the effect of sample self-shielding. It should be noted that a difference in the vibrational intensities, especially at low frequencies, can have an impact on the calculation of the Mean Square Displacement (MSD) and, consequently, on the estimation of the Debye Waller factor that is used in the calculation of the TCS within the multi-phonon expansion. In the present case, at a temperature of 20K, the average MSD from Eq. 1 and the AFGA model is 0.0647 \AA^2 for hydrogen atoms. While we could not find an experimental value to compare this result with, we note that in the case of biphenyl investigated in Ref.[32] at room temperature, the relative difference between the calculated and experimental MSDs was found lower than 20%, and the difference should decrease significantly at base temperatures.

Similarly, as anticipated, the total scattering cross section, $\sigma(E)$ for triptindane per formula unit was calculated using the AFGA approximation included within the NCrystal module [34], and it is reported in Figure 3 for

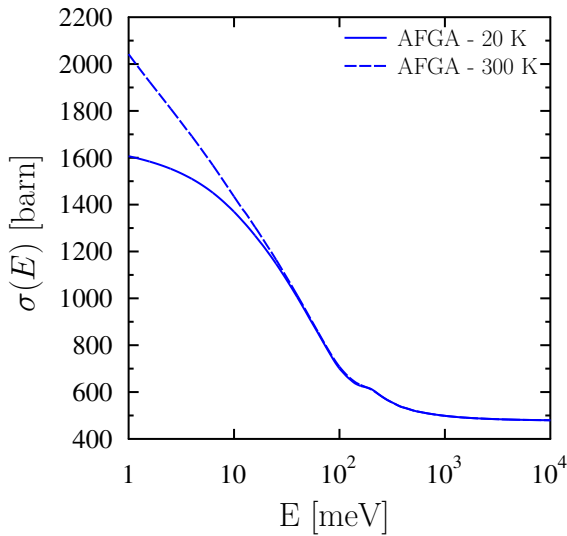


Figure 3. Total cross section per formula unit of triptindane obtained from the AFGA model, corresponding to a sample temperature of 20 K (solid blue line) and 300 K (dashed blue line) as a function of the incident neutron energy.

sample temperatures of both 20 K, similar to the one used for experiments on TOSCA, and 300 K. The low-temperature cross section is a clear example of how such function changes drastically as a function of the incident neutron energy, moving from the sum of free scattering cross sections, of hydrogens and carbons in the molecule, at epithermal neutron energies, to the (approximate) sum of bound scattering cross sections, of the same elements, in the cold-neutron energy limit. In the case of the room-temperature sample, it is also worth noting how the low-energy limit of $\sigma(E)$ deviates significantly from the sum of bound scattering cross sections, showing the temperature dependence of the total cross section at energies below tens of meV.

Finally, sample transmission spectra, $T(E)$, as a function of the incident neutron energy, E , were obtained from the AFGA total cross sections assuming values of the sample thickness, d , of 1 mm and 2 mm, and a bulk sample density of 1.2 g/ml. The results were computed via the Beer-Lambert law,

$$T(E) = \exp(-nd\sigma(E)), \quad (2)$$

with n the number density, and are shown in Figure 4.

3 Results

Once the AFGA-based synthetic values of $\sigma(E)$, $S(Q, \Delta E)$, and $T(E)$ were generated, they could be used as trial input files for the INSCorNorm algorithm, so as to calculate the self-shielding correction, $f(\theta, E, E_f)$. As discussed in detail in Ref.[25], the self-shielding correction for a flat-geometry sample and a forward-scattering angle θ_f can be approximated as [35]

$$f(\theta, E, E_f) = \frac{T(\theta = 0, E_i) - T(\theta = \theta_f, E_f)}{\log T(\theta = 0, E_i) + \log T(\theta = \theta_f, E_f)}, \quad (3)$$

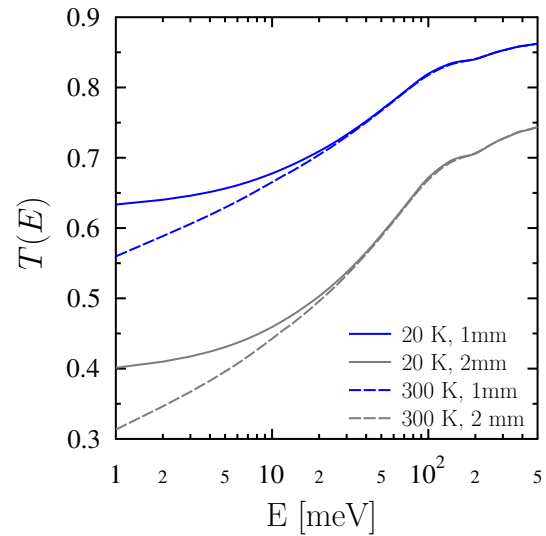


Figure 4. Sample transmission of a sample of triptindane, as obtained from the AFGA model, corresponding to a sample temperature of 20 K (solid lines) and 300 K (dashed lines), and to a sample thickness of 1 mm (blue lines) and 2 mm (gray lines) as a function of the incident neutron energy.

with

$$T(\theta, E) = \exp\left(\frac{\log T(E)}{\cos \theta}\right). \quad (4)$$

The computed self-shielding corrections for a sample at 20 K and thickness values of 1 mm (blue line) and 2 mm (gray line) are reported in Figure 5. In both cases, the correction causes a marked attenuation of the INS data, enhanced as the sample thickness increases and as the transmission decreases, as one can expect. As a function of the neutron-energy transfer on an indirect-geometry spectrometer, the correction is relatively flat above ca. 200 meV, while it decreases quickly as the energy decreases below ca. 150 meV. Therefore, one should take into consideration two main effects from the sample self-shielding. On the one hand, there is a significant - yet constant - contribution to the attenuation of the INS spectra related to the value of $T(\theta = \theta_f, E_f)$. As the final energy on indirect-geometry instruments is generally around few meV, one can appreciate that the transmission (total cross section) will be approximately at its minimum (maximum) within the dynamic range probed by the instrument. However, being constant in nature, such contribution does not spoil the comparison of the intensities of the experimental VDoS spectra with the ones from computer simulations and models. On the other hand, there is a contribution related to $T(\theta = 0, E)$, related to the incident neutron energy, that may change drastically over the dynamic range available on indirect-geometry INS spectrometers and that is responsible for the drop in the self-shielding correction below ca. 150 meV.

In order to visualise the effect of the self-shielding correction on INS spectra, Figure 6 shows the same synthetic spectrum reported in Figure 2 (dashed green line) together with the same spectrum multiplied by the self-

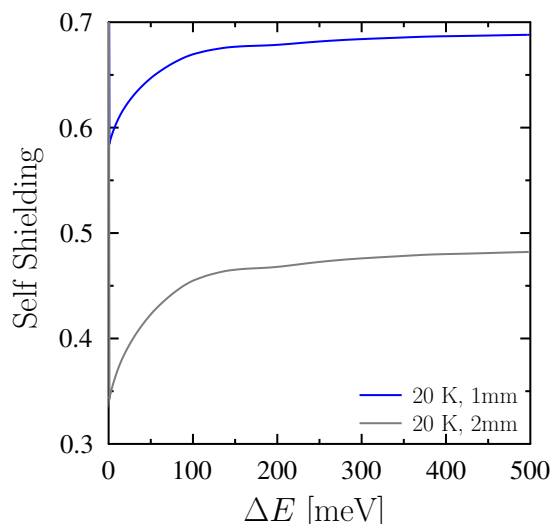


Figure 5. Self shielding correction, as a function of the neutron energy transfer, corresponding to a sample of triptindane, as obtained from the AFGA model, at a temperature of 20 K and for a sample thickness of 1 mm (blue line) and 2 mm (gray line).

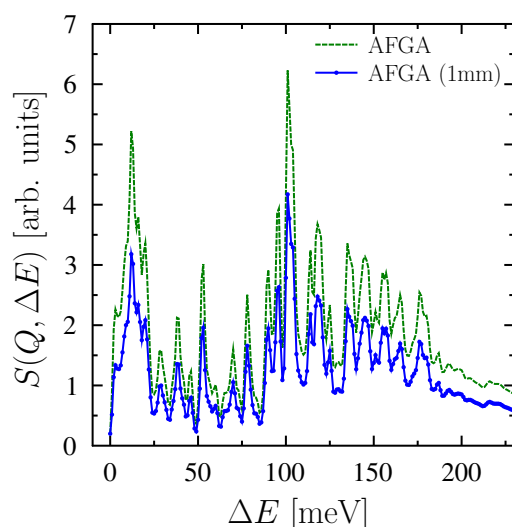


Figure 6. Synthetic INS spectra, as a function of the neutron energy transfer, corresponding to a sample of triptindane as obtained from the AFGA model (green line, the same as in Figure 2), and the same spectrum attenuated for the self shielding correction corresponding to a sample thickness of 1 mm (blue line with circles).

shielding correction for a 1-mm-thick sample at 20 K (blue line with circles). As already mentioned in the previous section, the effect of the attenuation becomes particularly relevant to the intensities of the low-energy modes, which undergo a suppression of about 15% in addition to the almost-constant suppression affecting the intensities at higher neutron energies.

4 Conclusions

In this work we have provided a worked example on how to implement the Average Functional Group Approximation within the INSCorNorm algorithm to obtain an accurate self-shielding correction of organic samples for which an experimental transmission spectrum is not available. We have quantified the effects of self-shielding in the case of triptindane at 20 K, corresponding, in the case of 1-mm-thick sample, to an additional 15% suppression of the low-energy vibrations to be added to the ca. 30% suppression affecting the vibrations above ca. 200 meV. Moreover, we have discussed how these corrections change depending on the sample thickness and temperature.

In conclusion, the inclusion of accurate sample self-shielding corrections for organic samples, as those available within the AFGA model, is a simple-yet-needed step for the comparison of experimental and theoretical vibrational densities of states, beyond the already successful interpretation of the vibrational energies, towards a quantitative assessment of the vibrational intensities as well.

The authors gratefully acknowledge Regione Lazio (G10795 published by BURL n. 69, 27/08/2019) and University of Rome Tor Vergata for the financial support to ISIS@MACH Regional Project. The Authors gratefully acknowledge the financial supports of the Consiglio Nazionale delle Ricerche - within CNR-STFC Grant Agreement [2014-2020 (n. 3420)] concerning collaboration in scientific research at the ISIS (UK) of STFC - and of the JRU ISIS@MACH ITALIA, Research Infrastructure hub of ISIS (UK) - MUR official registry U. 0008642.28-05-2020.

References

- [1] P.C.H. Mitchell, *Vibrational spectroscopy with neutrons: with applications in chemistry, biology, materials science and catalysis*, Vol. 3 (World Scientific, 2005)
- [2] F. Fernandez-Alonso, D.L. Price, *Neutron Scattering* (Academic Press, 2013)
- [3] K. Druzbicki, M. Gaboardi, F. Fernandez-Alonso, *Polymers* **13**, 1440 (2021)
- [4] V.F. Sears, *Neutron news* **3**, 26 (1992)
- [5] *ISIS neutron and muon source*, ISISNeutronandMuonSource, accessed July 2021
- [6] J. Granada, *Phys. Rev. B* **31**, 4167 (1985)
- [7] V. Laliena, J. Dawidowski, G. Cuello, J. Campo, *Nucl. Instrum. Meth. A* **993**, 165071 (2021)
- [8] J.M. Damian, D.C. Malaspina, J.R. Granada, *J. Chem. Phys.* **139**, 024504 (2013)
- [9] A. Hawari, I. Al-Qasir, V. Gillette, B. Wehring, T. Zhou, *Proc. PHYSOR 2004* pp. 25–29 (2004)
- [10] A. Hawari, *Nucl. Data Sheets* **118**, 172 (2014)
- [11] X.X. Cai, E. Klinkby, *New J. Phys.* **19**, 103027 (2017)
- [12] J. Wormald, A.I. Hawari, *Thermal neutron scattering law calculations using ab initio molecular dynamics*,

- in *EPJ Web Conf.* (EDP Sciences, 2017), Vol. 146, p. 13002
- [13] Y. Cheng, A.J. Ramirez-Cuesta, *J. Chem. Theory Comput.* **16**, 5212 (2020)
- [14] G. Romanelli, M. Krzystyniak, R. Senesi, D. Raspino, J. Boxall, D. Pooley, S. Moorby, E. Schooneveld, N. Rhodes, C. Andreani et al., *Meas. Sci. Technol.* **28**, 095501 (2017)
- [15] J.I. Robledo, J. Dawidowski, J.M. Damián, G. Škoro, C. Bovo, G. Romanelli, *Nucl. Instrum. Meth. A* **971**, 164096 (2020)
- [16] P. Ulpiani, G. Romanelli, D. Onorati, A. Parmentier, G. Festa, E. Schooneveld, C. Cazzaniga, L. Arcidiacono, C. Andreani, R. Senesi, *Rev. Sci. Instrum.* **90**, 073901 (2019)
- [17] L.R. Palomino, J. Dawidowski, J.M. Damián, G.J. Cuello, G. Romanelli, M. Krzystyniak, *Nucl. Instrum. Meth. A* **870**, 84 (2017)
- [18] S.C. Capelli, G. Romanelli, *J. Appl. Crystallogr.* **52**, 1233 (2019)
- [19] C. Andreani, R. Senesi, M. Krzystyniak, G. Romanelli, F. Fernandez-Alonso, *Riv. Nuovo Cimento* **41**, 291 (2018)
- [20] G. Romanelli, S. Rudić, M. Zanetti, C. Andreani, F. Fernandez-Alonso, G. Gorini, M. Krzystyniak, G. Škoro, *Nucl. Instrum. Meth. A* **888**, 88 (2018)
- [21] F. Cantargi, J. Dawidowski, C. Helman, J.I.M. Damian, R.J. Granada, G. Romanelli, J.G. Cuello, G. Skoro, M. Krzystyniak, *Validated scattering kernels for triphenylmethane at cryogenic temperatures*, in *EPJ Web Conf.* (EDP Sciences, 2020), Vol. 239, p. 14002
- [22] G. Škoro, G. Romanelli, S. Rudić, S. Lilley, F. Fernandez-Alonso, *Discovery of new neutron-moderating materials at isis neutron and muon source*, in *EPJ Web Conf.* (EDP Sciences, 2020), Vol. 239, p. 17008
- [23] L.R. Palomino, J. Dawidowski, C. Helman, J.M. Damián, G. Romanelli, M. Krzystyniak, S. Rudić, G.J. Cuello, *Nucl. Instrum. Meth. A* **927**, 443 (2019)
- [24] G. Romanelli, D. Onorati, P. Ulpiani, S. Cancelli, E. Perelli-Cippo, J.I.M. Damián, S.C. Capelli, G. Croci, A. Muraro, M. Tardocchi et al., *J. Phys. Condens. Mat.* **33**, 285901 (2021)
- [25] C. Scatigno, G. Romanelli, E. Preziosi, M. Zanetti, S.F. Parker, S. Rudic, C. Andreani, R. Senesi, *J. Chem. Theory Comput.* **16**, 7671 (2020)
- [26] D. Colognesi, *J. Neutron Res.* **19**, 147 (2017)
- [27] J. Vile, M. Carta, C.G. Bezzu, B.M. Kariuki, N.B. McKeown, *Polymer* **55**, 326 (2014)
- [28] A.M. Dilmaç, T. Wezeman, R.M. Bär, S. Bräse, *Nat. Prod. Rep.* **37**, 224 (2020)
- [29] R.S. Pinna, S. Rudić, M.J. Capstick, D.J. McPhail, D.E. Pooley, G.D. Howells, G. Gorini, F. Fernandez-Alonso, *Nucl. Instrum. Meth. A* **870**, 79 (2017)
- [30] S.F. Parker, L. Zhong, M. Harig, D. Kuck, *Phys. Chem. Chem. Phys.* **21**, 4568 (2019)
- [31] *Isis ins database*, <http://www.wisis2.isis.rl.ac.uk/INSdatabase/Theindex.asp>, accessed July 2021
- [32] P. Ulpiani, G. Romanelli, D. Onorati, M. Krzystyniak, C. Andreani, R. Senesi, *Nuovo Ciment. C* **44**, 1 (2021)
- [33] *Triptindane*, *pubchem identifier: Cid 12444533*, <https://pubchem.ncbi.nlm.nih.gov/compound/Triptindane>, accessed August 2021
- [34] K. Ramić, J.I.M. Damian, T. Kittelmann, D.D. Di Julio, D. Campi, M. Bernasconi, G. Gorini, V. Santoro, *Nucl. Instrum. Meth. A* **1027**, 166227 (2022)
- [35] A.K. Agrawal, *Phys. Rev. A* **4**, 1560 (1971)